

Diffuse Galactic antimatter from faint thermonuclear supernovae in old stellar populations

Roland M. Crocker^{1*}, Ashley J. Ruiter^{1,2}, Ivo R. Seitenzahl^{1,2,3}, Fiona H. Panther^{1,2}, Stuart Sim⁴, Holger Baumgardt⁵, Anais Möller^{1,2}, David M. Nataf^{1,6,7}, Lilia Ferrario⁸, J. J. Eldridge⁹, Martin White¹⁰, Brad E. Tucker^{1,2} and Felix Aharonian^{11,12}

Our Galaxy hosts the annihilation of a few 10^{43} low-energy positrons every second. Radioactive isotopes capable of supplying such positrons are synthesized in stars, stellar remnants and supernovae. For decades, however, there has been no positive identification of a main stellar positron source, leading to suggestions that many positrons originate from exotic sources like the Galaxy's central supermassive black hole or dark matter annihilation. Here we show that a single type of transient source, deriving from stellar populations of age 3–6 Gyr and yielding $\sim 0.03 M_{\odot}$ of the positron emitter ^{44}Ti , can simultaneously explain the strength and morphology of the Galactic positron annihilation signal and the Solar System abundance of the ^{44}Ti decay product ^{44}Ca . This transient is likely the merger of two low-mass white dwarfs, observed in external galaxies as the sub-luminous, thermonuclear supernova known as SN 1991bg-like.

First detected more than 40 years ago¹, the Galactic positron annihilation signal poses two central, unresolved challenges: (1) the development of an understanding of the absolute positron production rate in the Galaxy; and (2) the finding of an explanation for the gross morphology of the positron annihilation distribution across the Galaxy. In particular, historical measurements² have suggested a positron annihilation rate ~ 1.4 times larger in the Galactic bulge than in the Galactic disk, despite the bulge hosting $\lesssim 50\%$ the stellar mass³ and much less ($\lesssim 10\%$) recent star formation than the disk (see Supplementary Information).

This apparent strong positron emission from the bulge spurred the development of models in which positrons are injected by exotic sources such as the annihilation of dark matter or by the central supermassive black hole. However, severe gamma ray continuum constraints at energies^{4,5} $> 511 \text{ keV}$ imply that most Galactic positrons are injected into the interstellar medium (ISM) with kinetic energies $\lesssim 3 \text{ MeV}$. This has ruled out many explanations for the origin of positrons involving dark matter and others invoking diffuse, hadronic cosmic rays or compact positron sources such as pulsars². The energy constraint also means that the positrons' diffusive transport distance is less than or equal to a kiloparsec⁶ within their 10^5 – 10^6 yr lifetime in the ISM⁷. The positrons are therefore expected to annihilate relatively close to their injection sites, meaning that the Galaxy presents a thick target to the positrons on these spatial scales. Given that we also expect the annihilation of positrons in the Galaxy to be in a quasi-steady state (because the time between positron injection events is much less than the lifetimes of positrons in the ISM), then the Galactic production of positrons is in saturation. This implies that (1) the sky distribution

of annihilation radiation broadly reflects the distribution of positron sources and (2) the current positron injection rate into the ISM is equal to the annihilation rate inferred from the annihilation radiation flux.

The empirical situation regarding positron annihilation has recently undergone two important updates after a novel analysis⁸ of a larger dataset generated by the SPI spectrometer⁹ on the European Space Agency's INTEGRAL satellite: (1) the measured disk positron annihilation rate has been subject to a significant upwards revision after the detection of considerably more low surface brightness emission (implying a revised total Galactic positron annihilation rate of $5.0^{+1.0}_{-1.5} \times 10^{43} \text{ s}^{-1}$); and (2) the existence of a distinct, point-like Galactic centre source has been demonstrated with 5σ statistical significance¹⁰.

These new findings have important consequences for our understanding of Galactic positron production. Given the revision of the measured disk annihilation rate, the bulge (*B*) to disk (*D*) positron luminosity ratio is revised downwards to $B/D = 0.42 \pm 0.09$; this is equal, within error, to the ratio of the bulge to disk stellar mass³:

$$M_{\text{bulge}}/M_{\text{disk}} = (1.6 \pm 0.2) \times 10^{10} M_{\odot} / (3.7 \pm 0.5) \times 10^{10} M_{\odot} = 0.4 \pm 0.1$$

(see Supplementary Material). The effective angular resolution of the SPI observations of 2.7° (ref. ⁸) means that the point-like Galactic centre positron source encompasses the entire nuclear bulge¹¹ stellar population surrounding the supermassive black hole. The ratio of the positron luminosities of the nuclear bulge (*N*) to the bulge is

¹Research School of Astronomy and Astrophysics, Australian National University, Canberra 2611, Australia. ²ARC Centre of Excellence for All-Sky Astrophysics (CAASTRO), Canberra 2611, Australia. ³School of Physical, Environmental and Mathematical Sciences, UNSW Canberra, Australian Defence Force Academy, Canberra 2612, Australia. ⁴School of Mathematics and Physics, Queen's University, University Road, Belfast BT7 1NN, UK. ⁵School of Mathematics and Physics, University of Queensland, Brisbane 4072, Australia. ⁶Department of Physics and Astronomy, The Johns Hopkins University, Baltimore, Maryland 21218, USA. ⁷Center for Astrophysical Sciences, The Johns Hopkins University, Baltimore, Maryland 21218, USA. ⁸Mathematical Sciences Institute, Australian National University, Canberra 2601, Australia. ⁹Department of Physics, University of Auckland, Auckland 1010, New Zealand. ¹⁰Department of Physics, University of Adelaide, Adelaide 5005, Australia. ¹¹Dublin Institute for Advanced Studies, 10 Burlington Road, Dublin 4, D04 C932, Ireland. ¹²Max-Planck-Institut für Kernphysik, Saupfercheckweg 1, 69117 Heidelberg, Germany. *e-mail: rcrocker@fastmail.fm

$N/B = (8.3 \pm 2.1) \times 10^{-2}$ (ref. ⁸), again statistically equal to the ratio of the stellar masses of these structures:

$$M_N / M_{\text{bulge}} = (1.4 \pm 0.6) \times 10^9 M_{\odot} / (1.6 \pm 0.2) \times 10^{10} M_{\odot} = 0.09 \pm 0.04$$

Together, these facts imply that a single type of positron source connected to old stars could explain the global distribution of positron injection in the Galaxy—in contrast, putative exotic sources associated with the inner Galaxy, such as dark matter or the central super-massive black hole, cannot explain the disk positron signal.

Qualitatively, given the strong bulge signal, it has long been appreciated that a positron source connected to old stellar populations is preferred. For instance, ordinary type Ia (thermonuclear) supernovae (SNe Ia) have been a theoretically favoured, putative source of Galactic positrons^{2,12}. Alternatively, following older suggestions¹³, it was recently noted¹⁴ that flaring microquasars, also plausibly connected to old stars in some instances, seem capable of sustaining the Galactic positron annihilation rate.

However, the updated empirical situation now allows us to address the question of positron source age more quantitatively. To do this, we use the formalism of delay time distributions (DTDs; Fig. 1) and the known star formation histories of the bulge, disk and nucleus (Fig. 2) to find the positron source delay time t_p between star formation and the formation of a transient source that can reproduce the inferred B/D and N/B positron luminosity ratios. We adopt the parsimonious assumption (retrospectively justified by a global analysis of the data; see Supplementary Information) that the time-integrated efficiency for positron source creation per unit mass star formation is invariant throughout the Galaxy.

The blue and green bands in Fig. 3 show the modelled, current B/D and N/B ratios normalized to the observationally inferred positron injection ratios as a function of the positron source delay time t_p . Given that both bands show agreement of the model and observations for $t_p \approx 3$ –6 Gyr, we conclude that a single type of positron source, arising in stellar objects of this characteristic age and older, can explain the gross distribution of positron annihilation in the Galaxy.

But what is this source? We have already seen that positron injection energy constraints rule out many scenarios for positron creation. However, the required low injection energies are entirely compatible with a positron origin in the β^+ decay of radionuclides synthesized in stars and/or stellar explosions^{2,12}. Important positron-producing decay chains (with their markedly different total lifetimes shown in parentheses) are: $^{56}\text{Ni} \rightarrow ^{56}\text{Co} \rightarrow ^{56}\text{Fe}$ (~80 days); $^{44}\text{Ti} \rightarrow ^{44}\text{Sc} \rightarrow ^{44}\text{Ca}$ (~60 years); and $^{26}\text{Al} \rightarrow ^{26}\text{Mg}$ (~717,000 years). We consider each of these isotopes in turn.

Given the rates of SNe Ia and their prodigious yield of ^{56}Ni (~0.6 M_{\odot} per event), if only a few per cent¹⁵ of the positrons released in the $^{56}\text{Ni} \rightarrow ^{56}\text{Co} \rightarrow ^{56}\text{Fe}$ decay chain could reach the ISM, then they could sustain the total diffuse Galactic positron production¹². However, this explanation fails for two reasons: (1) the typical delay time of an SN Ia is too short to reproduce the observed Galactic annihilation line distribution (see Fig. 3 and ref. ²); and (2) recent analyses based on pseudo-bolometric SN Ia light curves constructed with the inclusion of infrared data (missing in earlier studies) indicate complete positron trapping in SN Ia ejecta to late times of $\gtrsim 800$ days^{16–18}, implying that very few positrons ($\ll 1\%$) escape to the ISM.

Similarly, the long decay time of ^{26}Al (comparable to the 10^5 – 10^6 year positron ISM thermalization timescale⁷) guarantees that the flux of the 1.809 MeV gamma ray line associated with ^{26}Al is in a steady state, whereas the total intensity of this line normalizes the total ^{26}Al production in the Galaxy to only $4 \times 10^{42} \text{ s}^{-1}$ (ref. ⁸), $\lesssim 10\%$ of the Galactic value. Moreover, the ^{26}Al emission is distributed along the Galactic plane, correlated with massive stars¹⁹, and does not match the overall annihilation morphology.

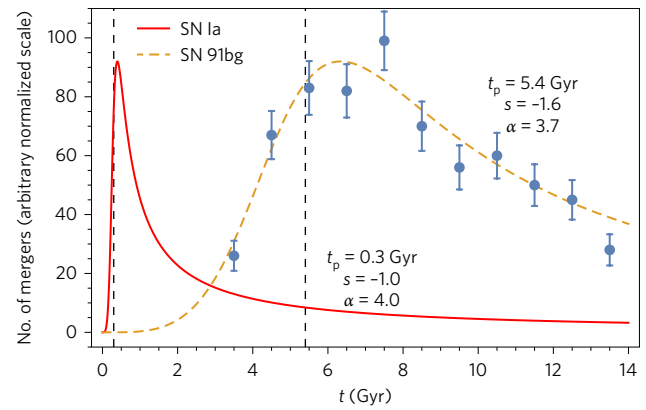


Figure 1 | Binned CO white dwarf-He white dwarf mergers within our BPS model. The data points with error bars given by $\pm\sqrt{N}$ together with DTD curves for SNe Ia and CO white dwarf-He white dwarf mergers (identified with SN 91bg-like events) are plotted as a function of time (increasing from the star formation event towards the present); the DTD curves are arbitrarily scaled in the vertical direction. The DTD returns $R_X[t]$, the rate of events of type X at epoch t (measured since the Big Bang) when convolved with the previous star formation history (SFH) of a region: $R_X[t] = v_X \int_0^t \text{DTD}[t-t'] \text{SFH}[t'] dt'$, where v_X is the number of events of type X that result from every solar mass of stars formed (see the Supplementary Information). We adopt a DTD of the form⁴⁴: $\text{DTD}[t] \propto [(t/t_p)^\alpha] / [(t/t_p)^{\alpha-s} + 1]$, where t_p is the characteristic delay time. For the SN Ia DTD, we set the parameters of the DTD function to be $t_p = 0.3$ Gyr, $s = -1.0$ and $\alpha = 4$ following ref. ⁴⁴. From fitting the BPS data on the CO white dwarf-He white dwarf mergers, we find (see Supplementary Information) that $t_p = 5.4^{+0.8}_{-0.6}$ Gyr, $s = -1.6^{+0.4}_{-0.5}$ and $\alpha = 3.7^{+1.2}_{-1.0}$ (1 σ errors). The vertical dashed lines are at 0.3 and 5.4 Gyr.

This leaves ^{44}Ti as the only viable radionuclide source of positrons. The fact that the $^{44}\text{Ti} \rightarrow ^{44}\text{Sc} \rightarrow ^{44}\text{Ca}$ decay chain has a 60 year decay time opens an interesting potentiality. On the one hand, such a decay time means that supernova ejecta have expanded to low densities before the daughter positrons are released and such positrons are extremely likely¹⁵ to reach the ISM. On the other hand, this decay time is considerably less than the positron ISM thermalization time, meaning that, depending on the recurrence time of Galactic ^{44}Ti sources, the total mass of ^{44}Ti in the Galaxy need not be in a steady state (even while the ISM daughter positrons of ^{44}Ti are in a steady state).

However, any ^{44}Ti scenario for Galactic positron production is also constrained by the following consideration. The observed abundance of ^{44}Ca relative to ^{56}Fe in Solar System material indicates that Galactic ^{44}Ti production at a look-back time $t_{\text{look-back}} > 4.55$ Gyr would have generated a positron luminosity of $(0.3\text{--}1.2) \times 10^{43} \text{ e}^+ \text{ s}^{-1}$ (refs ^{8,12,15}), $\lesssim 25\%$ of the current value. Thus if ^{44}Ti is currently the source of most positrons, the Galactic ^{44}Ti injection rate must be significantly larger now than between the Big Bang and the formation of the Solar System 4.55 Gyr ago. This requirement is naturally satisfied for ^{44}Ti sources that occur at roughly the same few Gyr delay times required by the Galactic distribution of positron annihilation.

As a further consideration, it is conventionally assumed that core-collapse supernovae deliver most of the ^{44}Ti in the Galaxy via alpha-rich freeze-out near the mass cut between the proto-neutron star and the ejecta. However, although evidence exists for the synthesis of a few $\sim 10^{-4} M_{\odot}$ of ^{44}Ti in three specific supernova remnants²⁰, the number of remnants currently emitting in the ^{44}Ti gamma ray and X-ray lines is too small to be a comfortable match to the number expected if such sources were responsible for most Galactic ^{44}Ca (ref. ²¹). Core-collapse nucleosynthesis models do not yield sufficient ^{44}Ti to explain the abundance of ^{44}Ca in mainstream, pre-Solar System material²².

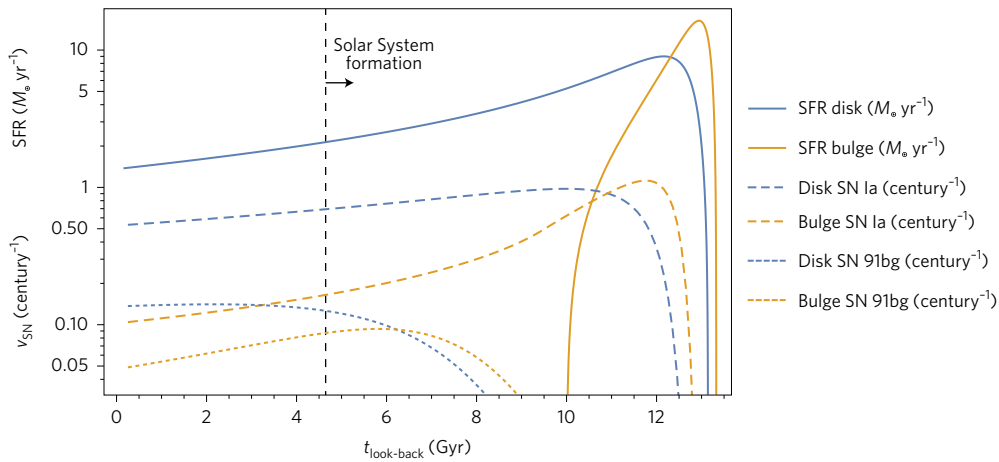


Figure 2 | SFRs of the disk and bulge adopted in this work and resulting SN Ia and SN 91bg formation rates v_{SN} . The data are plotted as a function of the look-back time (measured backwards from the present). The SFRs (solid lines) are plotted in $M_{\odot} \text{ yr}^{-1}$; the SN rates (dotted and dashed lines) are shown as rates per century. The SFRs are constrained to integrate (once the stellar mass loss is accounted for) to the existing stellar masses of the various regions and to match their stellar age distributions (see Supplementary Information). For the stellar masses, we adopt³ a current total stellar mass of the Milky Way of $(5.2 \pm 0.5) \times 10^{10} M_{\odot}$, a total mass in the bulge volume of $(1.6 \pm 0.2) \times 10^{10} M_{\odot}$ and a stellar mass in the disk outside the bulge volume of $(3.7 \pm 0.5) \times 10^{10} M_{\odot}$. The SFR in the bulge and disk both peaked 12–13 Gyr ago but, setting aside the nuclear bulge, the bulge has experienced negligible star formation since about 10 Gyr ago⁴⁰, whereas the disk has continued to host star formation at a rate of $\sim 1\text{--}2 M_{\odot} \text{ yr}^{-1}$ up until the present day. Note that the disk SN 91bg rate is the only illustrated rate currently increasing with cosmic time (the nuclear bulge SN 91bg rate, not shown here, is also currently increasing). The rates of occurrence of SNe are calculated using the formalism of DTDs (see the caption of Fig. 1) with $t_p = 0.3 \text{ Gyr}$ and $s = -1.0$ for SNe Ia and $t_p = 5.4 \text{ Gyr}$ and $s = -1.6$ for SNe 91bg.

The origin of pre-solar ^{44}Ca , which very likely derives from ^{44}Ti , is an important, unresolved problem in nuclear astrophysics.

A possible resolution of all these anomalies is that there are events, rarer than core-collapse supernovae, that supply significantly larger masses of ^{44}Ti than core-collapse supernovae seem capable of supplying²³. To comfortably obey the observational constraints (see Supplementary Information), these events should currently occur in the Galaxy every $\gtrsim 300 \text{ yr}$ (a few times longer than the decay time of the ^{44}Ti decay chain so that, as presaged earlier, the mass of ^{44}Ti in the Galaxy is not in a steady state so that neither is the ^{44}Ti gamma ray and X-ray line flux from the Galaxy steady) and they should also feature a minimum mean ^{44}Ti yield:

$$\left\langle M_{^{44}\text{Ti}} \right\rangle \gtrsim 0.013 M_{\odot} \left(\frac{R}{(300 \text{ year})^{-1}} \right) \left(\frac{\dot{N}_{e^{+}}}{5 \times 10^{43} \text{ s}^{-1}} \right) \quad (1)$$

Thus a universal, stellar positron source in the Galaxy that explains both the morphology and total amount of positron annihilation would: (1) occur at a characteristic delay time $\sim 3\text{--}6 \text{ Gyr}$ subsequent to star formation and would therefore be more frequent in today's Galactic disk than at early times; (2) would have a rate evolving according to this characteristic delay and would currently synthesize $5.8^{+1.3}_{-1.9} \times 10^{-5} M_{\odot} \text{ yr}^{-1}$ of ^{44}Ti (saturating the total Galactic positron luminosity minus that due to ^{26}Al decay); and (3) achieve this by yielding $\gtrsim 0.013 M_{\odot}$ of ^{44}Ti per event and occurring with a mean repetition time $\gtrsim 300 \text{ yr}$. Such a source would simultaneously explain the origin of pre-solar ^{44}Ca and naturally address the lack of strong ^{44}Ti gamma ray and X-ray line sources in the current sky.

This large ^{44}Ti yield can probably only be satisfied by astrophysical He detonations in which incomplete burning of ^4He leads^{24,25} to nucleosynthesis products dominated by intermediate mass alpha nuclei such as ^{40}Ca , ^{44}Ti and ^{48}Cr . Under optimum conditions, up to about one-third of the ^4He can be burned to ^{44}Ti for adiabatically compressed He white dwarf matter.

Our binary evolution population synthesis (BPS) models²⁶ using StarTrack²⁷ show an evolutionary channel that is expected to aggregate large masses of He at the high densities suitable for

detonation at long timescales after star formation. This channel (channel 3 in ref. ²⁶) involves low mass ($\sim 1.4\text{--}2.0 M_{\odot}$) interacting binary star systems that experience two mass transfer events (with only the second being a common envelope interaction), evolve into a carbon-oxygen (CO) white dwarf and a (pure) $0.31\text{--}0.37 M_{\odot}$ He white dwarf (with the progenitor of the latter never undergoing He core burning) and then subsequently merge (Fig. 4). These mergers occur at a characteristic timescale $t_p = 5.4^{+0.8}_{-0.6} \times 10^9 \text{ yr}$ (2σ). Non-trivially, this is an extremely good match to the empirical constraints on the characteristic delay time of a Galactic positron source (compare the vertical dashed lines on the right of Fig. 3).

It has previously been suggested^{28,29} that mergers of CO white dwarf–He white dwarf binaries may be the immediate progenitors of the class of sub-luminous thermonuclear supernova known as SN 1991bg-like (SN 91bg (ref. ³⁰)). The ^{56}Ni yields we estimate for our channel 3 merger events (Fig. 4) are a good match to the empirically determined ^{56}Ni yields of SNe 1991bg (but are too large to match SN 2005E-like supernovae, a class previously suggested³¹ to supply the Galactic positrons). The ^{56}Ni yields are estimated by assuming that the merger product assumes a transient configuration of quasi-hydrostatic equilibrium with the He white dwarf secondarily accreted on to the CO white dwarf primary before (1) the helium shell detonates and (2) the CO core detonates.

Empirically, SNe 91bg immediately match a number of our requirements: they are fairly frequent today, representing $\sim 15\%$ of all thermonuclear supernovae among the local galaxies sampled in the volume-limited Lick Observatory Supernova Search (LOSS³²) of 74 SNe Ia within 80 Mpc. They also occur in old stellar environments such as elliptical galaxies^{31,33}. The cosmological rate of SNe 91bg is increasing³⁴ (within large statistical uncertainties), suggesting that they are governed by delay times significantly larger than core-collapse SNe or SNe Ia (which are becoming less frequent in today's universe) as required by our scenario. In addition, SNe 91bg do show evidence of Ti in their spectra, as revealed by a characteristic Ti II absorption trough in their spectra around $\sim 4,200 \text{ \AA}$ (on this basis their potential importance for supplying Galactic ^{44}Ti decay positrons was previously noted¹²).

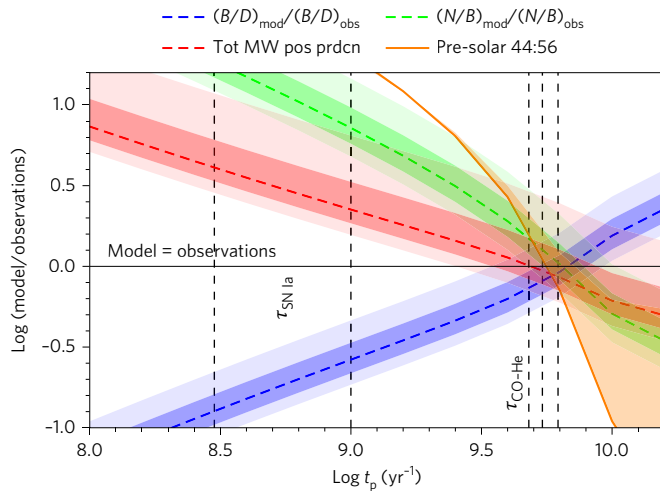


Figure 3 | Constraints on the characteristic delay time t_p of the main source of Galactic positrons. Curves plot the following quantities as a function of the delay time t_p : $(B/D)_{\text{mod}}/(B/D)_{\text{obs}}$ (blue curve), ratio of current modelled bulge to disk positron source occurrence divided by the observationally inferred⁸ ratio of bulge to disk positron luminosities 0.42 ± 0.09 ; $(N/B)_{\text{mod}}/(N/B)_{\text{obs}}$ (green curve), ratio of current modelled nucleus to bulge positron source occurrence divided by the observationally inferred⁸ ratio of nucleus to bulge positron luminosities $(8.3 \pm 2.1) \times 10^{-2}$; Tot MW pos prdcn (red curve), ratio of the modelled ^{44}Ti positron luminosity of the Milky Way to the observed non- ^{26}Al luminosity (central value $4.6 \times 10^{43} \text{ s}^{-1}$ (ref. ⁸) for $0.029 M_{\odot}$ ^{44}Ti per explosion and $f_{\text{SN91bg,bulge}} = 0.32$; and Pre-solar 44:56 (orange curve), ratio of the mass of ^{44}Ca to ^{56}Fe in pre-solar material divided by the observed⁵² value of 1.34×10^{-3} (negligible error) adopting a core-collapse and SN 91bg ^{56}Fe yield of $0.1 M_{\odot}$ and an SN Ia ^{56}Fe yield of $0.6 M_{\odot}$ and assuming (1) $0.029 M_{\odot}$ ^{44}Ti per SN 91bg (lower bound on band) and (2) $0.029 M_{\odot}$ ^{44}Ti per SN 91bg and, in addition, $1 \times 10^{-4} M_{\odot}$ ^{44}Ti per core collapse and $3 \times 10^{-5} M_{\odot}$ ^{44}Ti per SN Ia (upper bound on band). The heavy and light coloured bands cover the 1σ and 2σ uncertainties, respectively, in each measured quantity (except for the orange band which spans the systematic uncertainties in mean core-collapse and SN Ia ^{44}Ti production). The group of vertical lines labelled by $\tau_{\text{CO-He}}$ shows the central value and $\pm 1\sigma$ extent of the best-fit delay time for the CO white dwarf–He white dwarf mergers in the BPS model; the vertical lines at 300 and 1,000 Myr bracket τ_{SNIa} , the characteristic delay time for SNe Ia (ref. ⁴⁴); these occur at too short a delay time to explain the positron phenomenology.

Because SNe 91bg represent 10 of the 31 thermonuclear supernovae in early type galaxies in the LOSS sample^{32,35} and, spectrally, the bulge is an early type galaxy (of Hubble type² E0), we set the current bulge SN 91bg to the all SN Ia relative rate at $f_{\text{SN91bg,bulge}} = 0.32 \pm 0.16$ (2σ). We determine (see Supplementary Information) the rate of ordinary bulge SN Ia (excluding SN 91bg) to be $R_{\text{SNIa,bulge}} = 9.8 \times 10^{-2}$ /century from which $R_{\text{SN91bg,bulge}} = 4.6_{-2.7}^{+4.4} \times 10^{-2}$ /century. Given our assumption (retrospectively justified by an analysis of the data; see Supplementary Information) of a universal efficiency per unit stellar mass formed for creating positron sources (here understood to be SNe 91bg), we can then also calculate the current SN 91bg rate in the disk and the nuclear bulge as $(1.4 \pm 0.7) \times 10^{-1}$ /century and $(4.7 \pm 2.3) \times 10^{-3}$ /century, respectively, thus implying a SN 91bg Galactic recurrence time of $t_{\text{wait}} \approx 530 \text{ yr}$.

Integrating over disk supernova explosions up to 4.55 Gyr ago, we find that a mean ^{44}Ti yield $0.029_{-0.11}^{+0.18} M_{\odot} (f_{\text{SN91bg,bulge}}/0.32)$ is required to reproduce the observed abundance of ^{44}Ca relative to ^{56}Fe (from ^{56}Ni synthesized in SNe Ia and core-collapse SNe) for a characteristic delay time consistent with the other constraints (Fig. 3, orange curve). Adopting $M_{44\text{Ti}} = 0.029 M_{\odot}$ and the Galactic

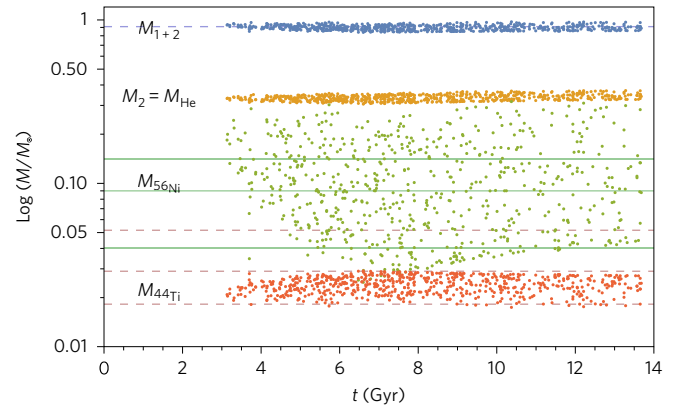


Figure 4 | Modelled white dwarf masses and inferred synthesized masses of ^{56}Ni and ^{44}Ti . The graph shows the modelled total (blue dots) and secondary (He; yellow dots) white dwarf masses at the time of merger and the inferred synthesized masses of ^{56}Ni (green dots) and ^{44}Ti (orange dots) versus delay time. We assume that the CO and He white dwarfs merge to form an object (of mean mass $0.91 M_{\odot}$, dashed blue line) that reaches quasi-hydrostatic equilibrium before exploding. For the ^{56}Ni yield we use the combined mass of both white dwarfs to which we apply an interpolation³⁵ of the modelled⁴⁹ mass of ^{56}Ni yielded in detonations of single, sub-Chandrasekhar white dwarfs; the steep dependence of the ^{56}Ni yield on the total mass is reflected in the scatter of the green points. The ^{56}Ni yields (mean $0.11 M_{\odot}$, $\sigma = 0.05 M_{\odot}$) are within the range of the observationally inferred⁵⁰ ^{56}Ni mass for a sample of 15 SNe 91bg (mean $0.09 M_{\odot}$, $\sigma = 0.05 M_{\odot}$, solid green lines). The ^{44}Ti yield of this channel, which depends on the amount of He in the correct density range ($\sim 10^5$ – 10^6 g cm^{-3}), is similarly estimated (see the Supplementary Information) at $(0.024 \pm 0.0028) M_{\odot}$ (1σ), consistent with the $0.029_{-0.11}^{+0.18} M_{\odot}$ determined in the main text for the Galactic positron source and shown as the dashed red lines.

SN 91bg rate already determined, we predict the current positron injection rate shown as the red curve in Fig. 3. This saturates, within errors, the absolute positron luminosity of the Galaxy (minus the positron luminosity of $4 \times 10^{42} \text{ e}^+ \text{ s}^{-1}$ due to ^{26}Al decay) within a t_p range consistent with the other constraints.

The mean ^{44}Ti yield per SN 91bg implied by this analysis, $\sim 0.03 M_{\odot}$, is close to the direct estimates we can make for CO white dwarf–He white dwarf mergers using our BPS data (Fig. 4), assuming a quasi-hydrostatic configuration, as seems to be warranted on the basis of our procedure for calculating the ^{56}Ni yield of the same explosions. It is also well within the range found for He detonation yields with nuclear network codes in single-zone simulations of explosive He burning: for $\sim 0.3 M_{\odot}$ of He with substantial admixtures of ^{12}C , ^{16}O or ^{14}N at a fixed density of 10^6 g cm^{-3} , temperatures $(2\text{--}4) \times 10^9 \text{ K}$ and using a 203 nuclide network, ref. ³¹ finds ^{44}Ti yields ranging up to $0.12 M_{\odot}$. In full numerical hydrodynamic calculations of the detonation of He shells of mass 0.15 – $0.3 M_{\odot}$ on top of CO white dwarf cores of mass 0.45 – $0.6 M_{\odot}$, ref. ³⁶ found ^{44}Ti yields of $(0.58\text{--}3.1) \times 10^{-2} M_{\odot}$. Adding N and C pollution into the He shell can act to significantly increase the ^{44}Ti yield (and decrease the ^{56}Ni yield) of the He detonation.

Our approach—to estimate the relevant nucleosynthesis yields by assuming that the merger remnant reaches hydrostatic equilibrium before detonating—appears viable, but awaits confirmation with high-resolution, three-dimensional numerical hydrodynamic simulations post-processed with a detailed nuclear network code. To our knowledge, no such simulation has been performed in the correct mass range to directly test our scenario and it is thus essentially an hypothesis that the CO–He white dwarf binary mergers detonate to yield ^{44}Ti masses in the range 0.013 – $0.03 M_{\odot}$; we commend such

simulations to the community. The considerations presented here do not constitute a logical proof that there is a single type of positron source in the Galaxy. A $\sim 10\%$ contribution⁸ from ^{26}Al from massive stars is inescapable; other sources such as microquasars^{13,14} plausibly make a further contribution. We have shown here, however, that the Galactic annihilation morphology admits of a single dominant positron source type, which must then be connected to stellar populations 3–6 Gyr old. This is a general constraint that is difficult to evade given the extreme paucity of young stars in the Galactic bulge, together with the fact that all regions of the Galaxy have old stellar populations.

Methods

Star formation rate parameterization. For the disk and bulge star formation rates (SFRs), we use the form suggested by ref.³⁷:

$$\log_{10}[SFR + D] = \max[Az^2 + Bz + C, 0] \quad (2)$$

The coefficients A , B , C and D for the disk are determined by fitting to the Milky Way disk star formation history data of ref.³⁸ renormalized so that the integrated stellar mass of the disk (outside the VVV volume) is $(3.7 \pm 0.5) \times 10^{10} M_{\odot}$ (ref.³); we find $\{A = -4.06 \times 10^{-2}, B = 0.331, C = 0.338, D = 0.771\}$ (note that we account for a factor 0.26 of the SFR lost to stellar winds and stellar ejecta³⁷). This parameterization gives a present day SFR in the disk of $1.4 M_{\odot} \text{ yr}^{-1}$, in tolerable agreement with previously published estimates (such as $1.65 \pm 0.19 M_{\odot} \text{ yr}^{-1}$ for a Kroupa initial mass function³⁹). For the current bulge region mass we require that the SFR, with the form given by equation (2), integrates to $1.55 \times 10^{10} M_{\odot}$ (ref.³), with the SFR peaking at a look-back time of 13 Gyr and reaching zero by 10 Gyr (ref.⁴⁰). With these constraints, the SFR can again be represented in the form of equation (2) with $\{A = -2.62 \times 10^{-2}, B = 0.384, C = -8.42 \times 10^{-2}, D = 3.254\}$. The bulge and disk star formation histories are plotted in Fig. 2.

For the star formation history of the nuclear bulge, the distinct population of stars that dominates the stellar density within 200–400 pc of the central supermassive black hole, there is intermittency and burstiness on various timescales⁴¹. However, averaging over $\gtrsim 100$ Myr, as pertinent to the calculation of the SN 91bg rate, nuclear star formation seems remarkably stable⁴². We therefore assume it to be constant at a rate equal to $0.14 M_{\odot} \text{ yr}^{-1}$, which will supply the mass of the nuclear bulge in the time since the Big Bang.

Delay time distribution. Our adopted DTD increases in proportion to t^{α} for times $t \ll t_p$ and asymptotes in proportion to t^s for times $t \gg t_p$ with the characteristic timescale t_p labelled as the delay time (and α and s parameters of the function describing the DTD). A population whose mergers are governed purely by gravitational radiation typically has $s = -1$ (ref.⁴³); if there are other processes hastening the process of inspiral, the DTDs are steepened, leading to $s < -1$. Following ref.⁴⁴ we set $\alpha = 4$, $s = -1$ and $t_p = 0.3$ Gyr for SN Ia (for these α and s values, the maximum rate of SN Ia occurs at $1.32 t_p$ subsequent to a star formation burst).

For the SN 91bg DTD, we set fiducial values of $s = -1.6$ and $\alpha = 3.7$ on the basis of fitting the data for CO white dwarf–He white dwarf mergers in our BPS (see Supplementary Fig. 1). Using a Markov chain Monte Carlo approach we fit (using the emcee package⁴⁵) the DTD functional form from ref.⁴⁴

$$\text{DTD} \propto \frac{(t/t_p)^{\alpha}}{(t/t_p)^{\alpha-s} + 1}$$

to the histogrammed BPS data. From this we obtain $t_p = (5.4^{+0.8}_{-0.6}) \times 10^9$ yr, $s = -1.6^{+0.4}_{-0.5}$ and $\alpha = 3.7^{+1.3}_{-1.0}$ (1σ errors). Note that in Fig. 3 we set $s = -1.6$ and $\alpha = 3.7$, but that t_p is a free parameter we scan over; we have checked that we obtain similar constraints when setting $s = -1.0$ and $\alpha = 4.0$.

Estimated ^{44}Ti and ^{56}Ni yields of He white dwarf–CO white dwarf mergers. Our estimates of the ^{44}Ti and ^{56}Ni yields of the He white dwarf–CO white dwarf mergers modelled within our BPS calculation are $\sim 0.03 M_{\odot}$ and $\sim 0.1 M_{\odot}$, respectively.

To obtain these yields, we have assumed that the merger product undergoes detonation. The efficiency with which the explosive nuclear burning converts initial He or CO into ^{44}Ti or ^{56}Ni is a function of density and temperature, and is also sensitive (in the case of He burning through to intermediate mass elements) to pollution of the He by C and/or N^{36,46}. Thus to estimate the yield of ^{44}Ti or ^{56}Ni by the CO white dwarf–He white dwarf mergers we need to know the density profile of the burning material and the fractional yield (of ^{44}Ti or ^{56}Ni) as a function of density (and temperature). In the relevant temperature range of a few $\times 10^9$ K, the efficient conversion of ^4He to intermediate mass elements (including ^{44}Ti) occurs when the ^4He is burned at a density between $\sim 10^5$ and 10^6 g cm^{-3} (ref.⁴⁶). The burning of CO through to ^{56}Ni requires that the CO is at densities higher than $\sim 10^7 \text{ g cm}^{-3}$ (we find that only a small contribution, $<10\%$, is made to the total ^{56}Ni from incomplete Si burning and He burning at lower densities).

To estimate the initial density profile of He (and CO) before it detonates, we assume that the merger remnant temporarily assumes a configuration of quasi-hydrostatic equilibrium with a total mass given by the combined mass of the pre-merger primary and secondary white dwarfs, with the He of the disrupted secondary white dwarf accreted into a shell on top of the primary CO white dwarf. This sort of approach is consonant with the suggestion⁴⁷ that relatively low-mass CO–CO white dwarf mergers first produce a merged remnant containing most of the aggregated mass of the binary before subsequently detonating. On the other hand, it is in tension with the pictures based on hydrodynamic merger simulations^{28,29}. In particular, the prompt detonation scenario²⁸ does not allow the assembly of $\gtrsim 0.1 M_{\odot}$ mass of ^4He in the correct density range for ^{44}Ti synthesis because detonation is triggered via He ignition shortly after mass transfer begins. The possibility of explosions at a later phase, shortly after the dynamic merger is complete, has previously been investigated²⁹ and a best match with SN 91 explosions has been suggested from the simulated merger of a $0.45 M_{\odot}$ He white dwarf with a $0.9 M_{\odot}$ CO white dwarf. This system is significantly more massive than the population of mergers identified in our BPS calculations and this model would yield only $\sim 3 \times 10^{-5}$ of ^{44}Ti , insufficient for our scenario. Thus we require that explosions occur in less massive mergers (and probably at later phases) than those explored previously^{28,29}.

We gain some confidence for this picture by considering the ^{56}Ni yields from the mergers, which we calculate in two ways. First, we produce an interpolation of the fractional ^{56}Ni yield of CO burning as a function of the initial density as presented in Fig. A1 of ref.⁴⁸. We then apply this parameterized yield to the CO–He merger remnant density profiles generated by assuming that the remnants reach hydrostatic equilibrium before detonating. Second, we use an existing interpolation³⁵ of the modelled⁴⁹ yield of ^{56}Ni in detonations of single, sub-Chandrasekhar white dwarfs given purely as a function of the total mass of the white dwarf. We find excellent agreement between these two approaches (see Supplementary Fig. 5). We then observe that, for our modelled distribution of CO white dwarf–He white dwarf mergers, applying either of these approaches, we derive ^{56}Ni yields that are very close to the observationally inferred ^{56}Ni yields of the sample of SNe 91bg assembled in ref.³⁰ (see caption to Fig. 4); this is an independent consistency check of our model.

We calculate ^{44}Ti yields from the He detonation in the merged He–CO remnants in a similar fashion to ^{56}Ni : (1) the initial He density profile is obtained assuming that the merger remnant achieves hydrostatic equilibrium before detonation; and (2) this density distribution is convolved with the fractional yield of ^{44}Ti from He detonation given as a function of density in ref.⁴⁶ (using our own interpolation of their results and adopting a fixed temperature of 2×10^9 K (ref.⁵¹)).

Data availability. The data that support the plots within this paper and other findings of this study are available from the corresponding author upon reasonable request.

Received 9 September 2016; accepted 12 April 2017;
published 22 May 2017

References

- Johnson, W. N. III, Harnden, F. R. Jr & Haymes, R. C. The spectrum of low-energy gamma radiation from the galactic-center region. *Astrophys. J. Lett.* **172**, 1–7 (1972).
- Prantzos, N. et al. The 511 keV emission from positron annihilation in the Galaxy. *Rev. Mod. Phys.* **83**, 1001–1056 (2011).
- Bland-Hawthorn, J. & Gerhard, O. The galaxy in context: structural, kinematic, and integrated properties. *Annu. Rev. Astron. Astrophys.* **54**, 529–596 (2016).
- Aharonian, F. A. & Atayan, A. M. On the origin of the galactic annihilation radiation. *Sov. Astron. Lett.* **7**, 395–398 (1981).
- Beacom, J. F. & Yüksel, H. Stringent constraint on galactic positron production. *Phys. Rev. Lett.* **97**, 071102 (2006).
- Alexis, A., Jean, P., Martin, P. & Ferrière, K. Monte Carlo modelling of the propagation and annihilation of nucleosynthesis positrons in the Galaxy. *Astron. Astrophys.* **564**, A108 (2014).
- Churazov, E., Sazonov, S., Tsygankov, S., Sunyaev, R. & Varshalovich, D. Positron annihilation spectrum from the Galactic Centre region observed by SPI/INTEGRAL revisited: annihilation in a cooling ISM? *Mon. Not. R. Astron. Soc.* **411**, 1727–1743 (2011).
- Siebert, T. et al. Gamma-ray spectroscopy of positron annihilation in the Milky Way. *Astron. Astrophys.* **586**, A84 (2016).
- Roques, J. P. et al. SPI/INTEGRAL in-flight performance. *Astron. Astrophys.* **411**, L91–L100 (2003).
- Skinner, G., Diehl, R., Zhang, X., Bouchet, L. & Jean, P. In *Proc. 10th INTEGRAL Workshop: A Synergistic View of the High-Energy Sky (INTEGRAL 2014)* 054 (2014); <http://pos.sissa.it/cgi-bin/reader/conf.cgi?confid=228>
- Launhardt, R., Zylka, R. & Mezger, P. G. The nuclear bulge of the Galaxy. III. Large-scale physical characteristics of stars and interstellar matter. *Astron. Astrophys.* **384**, 112–138 (2002).

12. Higdon, J. C., Lingenfelter, R. E. & Rothschild, R. E. The galactic positron annihilation radiation and the propagation of positrons in the interstellar medium. *Astrophys. J.* **698**, 350–379 (2009).
13. Guessoum, N., Jean, P. & Prantzos, N. Microquasars as sources of positron annihilation radiation. *Astron. Astrophys.* **457**, 753–762 (2006).
14. Siebert, T. *et al.* Positron annihilation signatures associated with the outburst of the microquasar V404 Cygni. *Nature* **531**, 341–343 (2016).
15. Chan, K.-W. & Lingenfelter, R. E. Positrons from supernovae. *Astrophys. J.* **405**, 614–636 (1993).
16. Leloudas, G. *et al.* The normal Type Ia SN 2003hv out to very late phases. *Astron. Astrophys.* **505**, 265–279 (2009).
17. Kerzendorf, W. E., Taubenberger, S., Seitenzahl, I. R. & Ruiter, A. J. Very late photometry of SN 2011fe. *Astrophys. J. Lett.* **796**, 26–30 (2014).
18. Graur, O. *et al.* Late-time photometry of Type Ia supernova SN 2012cg reveals the radioactive decay of ^{57}Co . *Astrophys. J.* **819**, 31 (2016).
19. Bouchet, L., Jourdain, E. & Roques, J.-P. The galactic ^{26}Al emission map as revealed by INTEGRAL SPI. *Astrophys. J.* **801**, 142 (2015).
20. Troja, E. *et al.* Swift/BAT detection of hard X-rays from Tycho's supernova remnant: evidence for titanium-44. *Astrophys. J. Lett.* **797**, L6 (2014).
21. The, L.-S. *et al.* Are ^{44}Ti -producing supernovae exceptional? *Astron. Astrophys.* **450**, 1037–1050 (2006).
22. Timmes, F. X., Woosley, S. E., Hartmann, D. H. & Hoffman, R. D. The production of ^{44}Ti and ^{60}Co in supernovae. *Astrophys. J.* **464**, 332–341 (1996).
23. Leising, M. D. & Share, G. H. Gamma-ray limits on galactic ^{60}Fe and ^{44}Ti nucleosynthesis. *Astrophys. J.* **424**, 200–207 (1994).
24. Hansen, C. J. Element production in simple helium burning. *Astrophys. J.* **169**, 585–588 (1971).
25. Woosley, S. E., Taam, R. E. & Weaver, T. A. Models for Type I supernova. I – detonations in white dwarfs. *Astrophys. J.* **301**, 601–623 (1986).
26. Karakas, A. I., Ruiter, A. J. & Hampel, M. R. coronae borealis stars are viable factories of pre-solar grains. *Astrophys. J.* **809**, 184 (2015).
27. Belczynski, K. *et al.* Compact object modeling with the StarTrack population synthesis code. *Astrophys. J. Suppl.* **174**, 223–260 (2008).
28. Pakmor, R., Kromer, M., Taubenberger, S. & Springel, V. Helium-ignited violent mergers as a unified model for normal and rapidly declining Type Ia supernovae. *Astrophys. J. Lett.* **770**, L8 (2013).
29. Dan, M., Guillochon, J., Brüggem, M., Ramirez-Ruiz, E. & Rosswog, S. Thermonuclear detonations ensuing white dwarf mergers. *Mon. Not. R. Astron. Soc.* **454**, 4411–4428 (2015).
30. Filippenko, A. V. *et al.* The subluminal, spectroscopically peculiar Type Ia supernova 1991bg in the elliptical galaxy NGC 4374. *Astron. J.* **104**, 1543–1556 (1992).
31. Perets, H. B. *et al.* A faint type of supernova from a white dwarf with a helium-rich companion. *Nature* **465**, 322–325 (2010).
32. Li, W. *et al.* Nearby supernova rates from the Lick Observatory Supernova Search – III. The rate-size relation, and the rates as a function of galaxy Hubble type and colour. *Mon. Not. R. Astron. Soc.* **412**, 1473–1507 (2011).
33. Howell, D. A. The progenitors of subluminal Type Ia supernovae. *Astrophys. J. Lett.* **554**, 193–196 (2001).
34. González-Gaitán, S. *et al.* Subluminal Type Ia supernovae at high redshift from the Supernova Legacy Survey. *Astrophys. J.* **727**, 107 (2011).
35. Piro, A. L., Thompson, T. A. & Kochanek, C. S. Reconciling ^{56}Ni production in Type Ia supernovae with double degenerate scenarios. *Mon. Not. R. Astron. Soc.* **438**, 3456–3464 (2014).
36. Waldman, R. *et al.* Helium shell detonations on low-mass white dwarfs as a possible explanation for SN 2005E. *Astrophys. J.* **738**, 21 (2011).
37. van Dokkum, P. G. *et al.* The assembly of Milky-Way-like galaxies since $z \sim 2.5$. *Astrophys. J. Lett.* **771**, L35 (2013).
38. Snaith, O. N. *et al.* The dominant epoch of star formation in the Milky Way formed the thick disk. *Astrophys. J. Lett.* **781**, L31 (2014).
39. Licquia, T. C. & Newman, J. A. Improved estimates of the Milky Way's stellar mass and star formation rate from hierarchical Bayesian meta-analysis. *Astrophys. J.* **806**, 96 (2015).
40. Nataf, D. M. The controversial star-formation history and helium enrichment of the Milky Way bulge. *Publ. Astron. Soc. Aust.* **33**, e023 (2016).
41. Krumholz, M. R., Kruijssen, J. M. D. & Crocker, R. M. A dynamical model for gas flows, star formation and nuclear winds in galactic centres. *Mon. Not. R. Astron. Soc.* **466**, 1213–1233 (2017).
42. Figer, D. F., Rich, R. M., Kim, S. S., Morris, M. & Serabyn, E. An extended star formation history for the galactic center from Hubble Space Telescope NICMOS observations. *Astrophys. J.* **601**, 319–339 (2004).
43. Ruiter, A. J., Belczynski, K. & Fryer, C. Rates and delay times of Type Ia supernovae. *Astrophys. J.* **699**, 2026–2036 (2009).
44. Childress, M. J., Wolf, C. & Zahid, H. J. Ages of Type Ia supernovae over cosmic time. *Mon. Not. R. Astron. Soc.* **445**, 1898–1911 (2014).
45. Foreman-Mackey, D., Hogg, D. W., Lang, D. & Goodman, J. emcee: the MCMC hammer. *Publ. Astron. Soc. Pacif.* **125**, 306 (2013).
46. Holcomb, C., Guillochon, J., De Colle, F. & Ramirez-Ruiz, E. Conditions for successful helium detonations in astrophysical environments. *Astrophys. J.* **771**, 14 (2013).
47. van Kerkwijk, M. H., Chang, P. & Justham, S. Sub-Chandrasekhar white dwarf mergers as the progenitors of Type Ia supernovae. *Astrophys. J. Lett.* **722**, 157–161 (2010).
48. Fink, M. *et al.* Double-detonation sub-Chandrasekhar supernovae: can minimum helium shell masses detonate the core? *Astron. Astrophys.* **514**, A53 (2010).
49. Sim, S. A. *et al.* Detonations in sub-Chandrasekhar-mass C+O white dwarfs. *Astrophys. J. Lett.* **714**, 52–57 (2010).
50. Sullivan, M. *et al.* The subluminal and peculiar Type Ia supernova PTF 09dav. *Astrophys. J.* **732**, 118 (2011).
51. Moore, K., Townsley, D. M. & Bildsten, L. The effects of curvature and expansion on helium detonations on white dwarf surfaces. *Astrophys. J.* **776**, 97 (2013).
52. Lodders, K. Solar System abundances and condensation temperatures of the elements. *Astrophys. J.* **591**, 1220–1247 (2003).

Acknowledgements

R.M.C. was the recipient of an Australian Research Council Future Fellowship (FT110100108). Parts of this research were conducted by the Australian Research Council Centre of Excellence for All-sky Astrophysics through project number CE110001020. D.M.N. is supported by the Allan C. and Dorothy H. Davis Fellowship. The authors thank J. Avila, J. Beacom, N. Bell, G. Bicknell, D. Clayton, K. Freeman, O. Gerhard, J. Hurley, T. Ireland, A. Karakas, M. Kerr, J. Machacek, F. Melia, D. Murtagh, R. O'Leary, R. Pakmor, T. Siebert, P. Tisserand, R. Volkas, A. Wallner, R. Wyse and F. Yuan for very useful discussions. They particularly thank B. Schmidt for pointing out the potential importance of SN1991bg-like SNe to the positron problem.

Author contributions

All the authors discussed the results and commented on the manuscript. R.M.C. wrote the paper. A.J.R. performed the BPS modelling and provided theoretical input. I.R.S. provided theoretical input, helped with calculating the yields of the helium detonations and contributed to the writing of the paper. F.H.P., A.M. and B.E.T. provided advice about the rates, prevalence and distribution of 91bg in supernova searches. H.B., L.F. and J.J.E. provided advice on the BPS modelling. A.M. and M.W. provided statistical analysis. D.M.N. provided advice about the star formation history of the Galactic bulge and other theoretical input. S.S. provided input on the phenomenology of SN explosions. F.A. provided input on the phenomenology of positron transport and annihilation radiation. All the authors commented on the draft text.

Additional information

Supplementary information is available for this paper.

Reprints and permissions information is available at www.nature.com/reprints.

Correspondence and requests for materials should be addressed to R.M.C.

How to cite this article: Crocker, R. M. *et al.* Diffuse Galactic antimatter from faint thermonuclear supernovae in old stellar populations. *Nat. Astron.* **1**, 0135 (2017).

Publisher's note: Springer Nature remains neutral with regard to jurisdictional claims in published maps and institutional affiliations.

Competing interests

The authors declare no competing financial interests.